Ife Social Sciences Review
Faculty of Social Sciences,
Obafemi Awolowo University Ile Ife, Nigeria
Journal homepage: www.issr.oauife.edu.ng/journal
ISSN:0331-3115 eISSN:2635-375X

Estimation of Soil Carbon and Spatial Variability of Soil Properties in Omo Biosphere Reserve, Ogun State, Nigeria

Mshelia Z. H.[1, 2], Aigbokhan O.J.[2]
[1]Institute of Life and Earth Sciences (including Health and Agriculture), Pan African University, University of Ibadan, Nigeria
[2]Department of Environmental Modelling and Biometrics, Forestry Research institute of Nigeria, Ibadan

Abstract

Understanding the role of soil in climate change mitigation requires accurate estimates of soil carbon. Soil Organic Carbon (SOC) plays a vital role in mitigating global climate change, and alleviates land degradation and enhances crop production and food security. Soil samples were collected with soil auger from 25 sample plots (30 m x 30 m) at depths of 0 – 15 cm in Omo Biosphere Reserve. The quantity of SOC per hectare was determined using a bulk density measurement. To examine the spatial variance of soil parameters, descriptive statistics and Kriging spatial interpolation techniques were employed. The estimated quantity of soil organic carbon in the Omo biosphere spans from 9.89 to 76.61 ton/ha with a mean of 29.14 ton/ha, whereas the estimated amount of CO_2 sequestered ranges from 36.31 to 281.15 ton/ha with a mean of 106.94 ton/ha. The estimated total content of the SOC in the biosphere reserve was 11,801.43 tons, while the CO_2 equivalent is 43,311.25 tons. Due to varying nuggets to sill ratios, the soil properties displayed varied spatial dependence. Strongly spatially dependent were OM, N, Cu, Na, and K, somewhat spatially dependent were Mn, Fe, Mg, Sand, and Clay and weakly spatial dependent were OC, pH, P, Zn, Ca, Silt and CEC. The study concluded that monitoring soil degradation through details soil mapping is an important step in reducing emission and enhancing soil carbon sequestration.

Keywords: Climate change, Bulk density, Kriging, Interpolation, Soil degradation

Introduction

A vital natural resource that is essential to the food production is soil (Buol *et al.*, 2003). Climate, vegetation or other organic matter, geology, local topography, and time were listed as environmental factors that influence soil (Ezeaku, 2011). Healthy soils are crucial for sustaining the growth of both natural and managed vegetation, as well as other ecosystem functions such as climate regulation and oxygen production. They also provide feed, fiber, fuel and other materials for making medications (FAO, 2015). The links between soils and vegetation is reciprocal. Plant develops more quickly in fertile soil because it supplies them nutrients, serves as a reservoir for their water, and provides the substrate for their roots to attach to. By stabilising the soil, preserving the water and nutrient cycle and lowering water and wind erosion, vegetation, tree cover, and forests in turn prevent soil deterioration and desertification (FAO, 2015). Regarded as the main cause of global warming, carbon dioxide (CO_2) is one of the main greenhouse gases, accounting for 72% of anthropogenic greenhouse gases (IPCC, 2007). According to estimates, 9–26% of the global greenhouse effects are caused by CO_2 (Kiehl, *et al.*, 1997). From 280 parts per million (ppm) in the pre-industrial period (1750) to 408.84 ppm in July 2017, a rise of 2.11 ppm per year has been seen in the atmospheric CO_2 concentration (NOAA, year?). The main cause of this significant increase in CO_2 concentration level in

the atmosphere is attributed to anthropogenic activity (Ahmed, 2018). The soil C pool is approximately four times bigger than the atmospheric C pool globally, and variations in the soil CO_2 content have impact on the equilibrium of the atmospheric CO_2 (Luo, *et al.*, 2006). Even though forests cover just 30 % of the planet's surface, they contain more than two-thirds of the world's soil organic carbon stock, making them the most carbon-rich terrestrial ecosystems (Ahmed, 2018). Using photosynthesis to fix atmospheric carbon into plant tissues, plant litter is then released into the soil. A fraction of this C is retained in soils, while the majority is released to the atmosphere as a result of soil respiration. Some of the stored C in soil can be sequestrated as soil organic matter and/or humus for as long as a million years (Cheng, *et al.*, 2007). Although measuring soil pararameters can be expensive and time consuming, it is possible to estimate their anticipated values in places where observations are not possible by using geostatistical and spatial interpolation techniques, in particular (Goovarerts, 1999; Pebesma, 2006 and Krasilnikov, *et al.*, 2008). Therefore, geostatistics involves the analysis and interpretation of any spatially referenced data (Hengl, 2009) and the estimation and modelling of spatial correlation (Biv, *et al.*, 2008). Its advantage is that it predicts both geographical trends and spatial correlations and identifies spatial variability at both large and small scales (Cressie, 1993). To provide the most precise and objective findings for each situation at hand, it is crucial to select the most suitable geostatistical models and methodologies. environmental sciences frequently employ geostatistics (Hengl, 2009; Goovaerts, 1997; Li, *et al.*, 2008 and Li, *et al.*, 2014)

Materials and Method

Study Area

Omo Forest Reserve, which derives its name from the River Omo that traverses it, is located between latitudes 6º 42' to 7º 05' N and longitude 4º 12' and 4º 35' E (Fig. 1) in Ogun state South-western Nigeria. Omo covers about 130,500 hectares, which includes a 460 ha Strict Nature Reserve established in 1977 known Omo Biosphere (Okali and Ola-Adams 1987). The climate is tropical, and it is characterized by wet (February to November) and dry (December and January) seasons. The temperature ranges between 21^0 and 34^0C while the annual rainfall ranges between 150 and 3000 mm (Larinde *et al*., 2011; Adedeji *et al*., 2015).

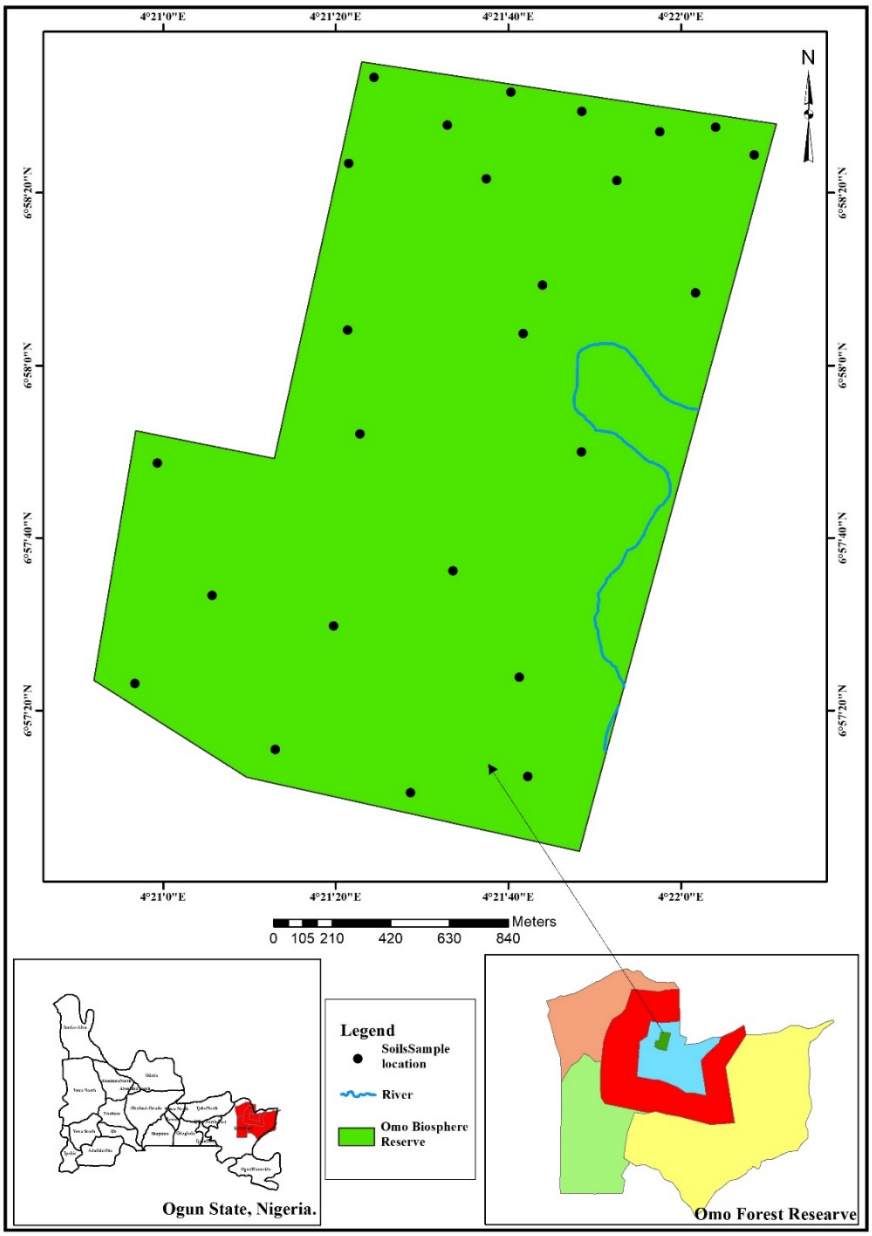

Figure 1. Omo Forest Reserve Showing the Study Area

In the Omo Biosphere Reserve in 2018, during the dry season, soil samples were taken from 25 sample plots (30 m x 30 m). Within each sample plot, a diagonal line was created, and soil samples were taken at the two ends and in the middle of the line. Using a soil auger, four soil cores were used to obtain soil samples from 0 – 15 cm in depth. Each plot of soil samples were properly mixed, and composite samples were taken, kept in polythene bags and labelled appropriately for laboratory analysis. Soil samples were air dried and put through a 2 mm sieve.

Bulk density.

The bulk density of the samples was determined by the test for bulk density: oven-dry a sample of known volume to remove all moisture and weigh it. The bulk density is the dry weight in grams divided by the volume in cubic centimeters.

$$\text{Unit bulk density} = \frac{\textbf{\textit{Unit weighted sample}}}{\textbf{\textit{Unit volume of sample}}} \quad (1)$$

Soil Carbon Estimation

A proportion of the total soil organic carbon is often reported through soil testing for organic carbon. The quantity of carbon per hectare in a specific depth of soil was estimated using a measure of bulk density. The proportion of organic carbon in soil, represented as a unit of carbon value, and the bulk density, measured in grams per cubic meter.

% of soil organic carbon x Bulk density ($g/cm^{3)}$ x Soil depth (cm) (2)

Descriptive statistics

Descriptive statistics including mean, median, standard deviation, coefficient of variation, minimum, maximum, skewness (skew), and kurtosis, were used to calculate the soil properties. Skewness and kurtosis of the data were used to test for normality for each of the soil properties in the R programming language. logarithmic transformation was applied to some of the data that did not pass the normality test (OC, OM, N, Na, and K). The variability of the soil properties was interpreted using the coefficient of variation (CV) and classified into most (CV: >35%), moderate (CV: 15-35%) and least (CV: <15%) variable ranges (Wilding, 1985).

Geostatistical Analysis

For this study, the ordinary kriging method was employed. It uses a linear geostatiscal interpolation method. The sums of the neighbouring sampled concentrations were used to construct Kriging estimations. The following equation was employed to compute it (Wang 1999):

$$Z^*(x_0) = \sum_{i=l}^{n} \lambda_i z(x_i) \quad (3)$$

Where:

$Z^*(x_0)$ = *is the predicted value at position* x_0

$z(x_i)$ = *the known value at sampling site* x

λ = *the weighting coefficient of the measured site, and*

n = *is the number of sites within the neighbourhood searched for the interpolation.*

Semivariogram modelling and estimation, akin to fitting a least line in regression analysis are crucial for structural analysis and spatial interpolation (Chen, *et al*, 2017). To pinpoint the best-fit model for each soil attribute, estimate of semi-variogram models including stable, gaussian, exponential, circular and spherical, were made. The intrinsic and regionalised variable theories allow for the expression of a semivariogram as shown below (Nielsen and Wendroth, 2003):

$$\gamma(h) = \frac{1}{2N(h)} \sum_{i=1}^{N(h)} [z(x_i) - z(x_i + h)]^2 \quad (4)$$

Where:

$\gamma(h)$ = *is the semivariance*

h = *the lag distance*

z = *the parameter of the soil property*

$N(h)$ *= the number of pairs of locations separated by a lag distance* h

$z(x_i)$ *and* $z(x_i+h)$ *= are values of* z *at* x_i *and* x_i+h *(Wang and Shao2013).*

The empirical semi-variograms obtained from the data were fitted by theoretical semi-variogram models to produce geostatistical parameters, including nugget variance (c_0), structured variance (c_1), sill variance (c_0+c_1), and distance parameter (k). The nugget/sill ratio, $c_0/(c_0+c_1)$ was calculated to characterize the spatial dependency of the values. In general, a nugget/sill ratio <25 % indicates strong spatial dependency and >75 % indicates weak spatial dependency; otherwise, the spatial dependency is moderate (Cambardella, *et al*.1994).

Cross Validation

The cross-validation technique was performed to choose the best fitted semi-variogram model for each of the studied soil properties, that is, by comparing the estimated values which were kriged by using the semi-variogram model with the actual values. Thus, for each sampled location, the collected observations included the measured value, $Z(x_i)$ and the estimated value, $Z'(x_i)$, as well as their standard values of $Z_1(x_i)$ and $Z_2(x_i)$. The performance statistics were assessed in terms of mean error (ME), Average Standard Error (ASE), Root Mean Square Error (RMSE), Mean Standard Error (MSE), Root Mean Square Standardized Error (RMSSE) (Yang, *et al*, 2011) and expressed in equation 5-9.

$$ME = \frac{1}{N}\sum_{i=1}^{N}[Z(x_i) - Z'(x_i)] \quad (5)$$

$$MSE = \frac{1}{N}\sum_{i=1}^{N}[Z_1(x_i) - Z_2(x_i)] \quad (6)$$

$$ASE = \sqrt{\frac{1}{N}\left[\sum_{i=1}^{N} Z'(x_i) - \left(\sum_{i=1}^{N} Z'(x_i)\right)/N\right]^2} \quad (7)$$

$$RMSE = \sqrt{\frac{1}{N}\sum_{i=1}^{N}\left[Z(x_i) - Z'(x_i)\right]^2} \quad (8)$$

$$RMSSE = \sqrt{\frac{1}{N}\sum_{i=1}^{N}\left[Z_1(x_i) - Z_2(x_i)\right]^2} \quad (9)$$

Where:

$Z(x_i)$ *= measured value*

$Z'(x_i)$, *= the estimated value*

$Z_1(x_i)$ *= standard value*

N = number of observations

If ME of the model equals 0, ASE equals RMSE, MSE equals 0, RMSSE equals 1(Yang, *et al*, 2011). This indicates that the interpolation is method unbiased based on ME value of zero or close to zero and the goodness of fit accuracy on Kriging algorithm based on the value of ASE equals RMSE.

Results and Discussion

Estimation of Soil Organic Carbon

The estimated amount of soil organic carbon in the Omo biosphere ranges from 9.89 to 76.61 ton/ha, with a mean of 29.14 ton/ha, while the range per plot was 0.89 to 6.89 ton/plot (900m^2), with mean of 2.62 ton/plot (Table 1). The CO_2 sequestered ranges from 36.31 to 281.15 ton/ha and 3.27 to 25.30 ton/plot, with a mean of 106.94 ton/ha and 9.62 ton/plot respectively (Table 1). Omo Biosphere Reserve covered 420 ha and included 15 ha of water bodies. Therefore, the actual area covered by forest and open space was 405 ha. The estimated total content of the organic soil carbon in the biosphere reserve was 11,801.43 tons, while the CO_2 equivalent is 43,311.25 tons. Soils are a major source of carbon emissions aside from deforestation. The soil carbon pool is the largest and most active carbon pool in terrestrial ecosystems and is an important source of atmospheric greenhouse gases (Wang *et al*. 2021). The global soil organic carbon (SOC) pool is about 1,550 Pg, which is twice the atmospheric carbon pool and three times the biological carbon pool (Lal, 2004). Thus, slight changes in the SOC pool will significantly affect the atmospheric carbon content; for example, a change of only 10% of the SOC pool is equivalent to 30 years of CO_2 releases caused by human activities (Kirschbaum, 2000). In addition, a slight increase in the rate of soil carbon oxidation caused by an increase in temperature will increase the atmospheric CO_2 concentration (Davidson and Janssens, 2006). Makinde, *et al.*, (2017) reported 5.8 tons of soil organic carbon in Oluwa Forest Reserve South Western Nigeria. Although, it was lower than the SOC reported in this study, it is significant in increasing the capacity of the forest to sink carbon. Soil carbon sequestration plays an important role in mitigating anthropogenic increases in atmospheric CO_2 concentrations. Favourable climate conditions, particularly high precipitation, tend to increase both species richness and belowground biomass, which has a consistent positive effect on SOC storage in forests, shrublands, and grasslands (Chen *et al.*, 2018). The high species diversity of Omo Biosphere Reserve explained why soil organic carbon contributed significantly to the reserve's capacity to sequester carbon. Ecosystem management that maintains high levels of plant diversity enhances SOC storage and other ecosystem services that depend on plant diversity. As a result, in any carbon study, soil carbon must always be considered.

Table 1. Summary of Soil Carbon Estimation from the Sample Plots

Parameter	% soil C	Soil C (t/ha)	Soil C (t/plot)	CO_2 (t/ha)	CO_2 (t/plot)
Mean	1.7372	29.13932	2.622539	106.9413	9.624717
Minimum	0.6	9.8928	0.890352	36.30658	3.267592
Maximum	3.98	76.60704	6.894634	281.1478	25.30331

Variability of Soil Properties

Table 1 shows the descriptive statistics of the studied soil properties. The soil was acidic with pH ranging between 4.81 to 6.07 and average of 5.48. According to the rating of Esu (1991) the soil nutrients are classified into low, medium and high. The organic carbon and matter content of the soil ranged between 0.6% and 3.98% with a mean of 1.74% and 1.03% and 6.86% with mean of 3.04%, respectively. The status of the organic carbon was low, while the organic matter was moderate. The mean nitrogen of 0.14% was low, while phosphorus with mean value of 4.85 mg/kg was moderate. Manganese (Mn), iron (Fe), copper (Cu) and zinc were high with mean value of 27.65 mg/kg, 53.84 mg/kg, 3.51 mg/kg and 81.52 mg/kg respectively. The high content of (Zn) of Mn, Fe, Cu and Zn was due to the acidity of the soil that encourage the uptake of micronutrients. The concentration of potassium (K) was low with mean of 0.0015 Cmol/kg, moderate concentration of sodium (Na) with mean of 1.64 Cmol/kg whereas, magnesium (Mg), calcium (Ca), and Cation Exchange Capacity (CEC) was in the study. The Coefficient of Variation (CV) ranged from 6.23% in pH to 392.23% in K. The range of CV for the soil sampling locations suggested different degrees of heterogeneity among the soil properties studied.

Soil Properties Spatial Distribution

The distribution of the soil chemical properties, OC, OM, N, P, Na and K was not normal due to the greater degrees of skewness and kurtosis, as shown in Table 2. After applying a logarithm transformation to the data sets to reduce the skew and kurtosis values, the altered data sets were employed in the spatial analysis, as shown in Figure 2 a-r. The parameters of the analysed soil attributes' model fitting and semi-variance analysis are shown in Figures 2 a-r and Table 3. for their notable match to the soil characteristics, various theoretical semi-variogram models were shown. the semi-variogram of pH, P, Na, K, Mg, Ca, sand, clay and silt best fits an exponential model. The semi-variograms of OM, Cu Zn and CEC, were best fitted by the Gaussian model; OC and N by the stable model; and Fe by the spherical model. According to previous studies' findings, the exponential model best captures the spatial variability in soil chemical properties since it explains the most variance in the dataset (Reza *et al.*, 2010., Venteris *et al.*, 2013, Bhunia *et al.*, 2016, Lark, 2000., Tripathi *et al.*, 2015., Panday *et al.*, 2018).

Table 2. Descriptive statistics of the studied soil properties

Parameter	Mean	Median	SD	Min	Max	CV (%)	Skew Ness	Kurtosis	Skew ness (LT)	Kurtosis (LT)
Ph	5.48	5.53	0.34	4.81	6.07	6.23	-0.29	-0.68		
O.C (%)	1.74	1.42	0.83	0.60	3.98	48.19	1.25	1.19	0.21	-0.01
O.M (%)	3.04	2.58	1.42	1.03	6.86	46.85	1.22	1.2472	0.10	0.154
N (%)	0.142	0.12	0.07	0.05	0.34	48.50	1.36	2.13	-0.05	0.40
P (mg/kg)	4.85	4.47	2.01	2.40	11.23	41.45	1.44	2.96	0.28	0.06
Mn (mg/kg)	27.65	28.50	13.94	2.00	52.70	50.43	-0.25	-0.629		
Fe (mg/kg)	53.84	47.00	27.21	7.00	111.00	50.54	0.34	-0.66		
Cu (mg/kg)	3.51	3.40	1.47	0.80	6.70	41.93	0.17	0.13		
Zn (mg/kg)	81.52	74.00	26.96	40.00	134.00	33.07	0.31	-0.94		
Na (Cmol/kg)	1.64	1.09	1.93	0.31	8.58	118.14	3.16	9.37	1.45	3.82
K (Cmol/kg)	0.01	0.01	0.01	0.01	0.031	392.23	4.99	24.96	3.67	15.92
Mg (Cmol/kg)	4.84	4.59	2.19	0.74	9.79	45.19	0.79	0.83		
Ca (Cmol/kg)	9.81	9.88	4.034	4.49	20.06	41.128	0.7161	0.29		
Sand (%)	77.94	76.50	5.46	70.50	92.50	7.01	0.89	0.88		
Clay (%)	12.14	11	3.16	7.00	19.00	26.04	0.24	-0.25		
Silt (%)	10.16	10.5	4.05	0.50	16.50	39.84	-0.35	-0.13		
CEC (Cmol/kg)	16.28	16.29	4.64	9.37	26.41	28.49	0.45	-0.66		

Nugget to sill ratio of <0.25 indicates strong spatial dependence due to the intrinsic (inherent) factors such as soil texture and mineralogy, while a ratio between 0.25 and 0.75 indicates moderate spatial dependence due to extrinsic and intrinsic factors, and a ratio >0.75 indicates weak spatial dependence due to the extrinsic factors such as fertilization and tillage (Cambardella *et al.*, 1994). Because of the nugget to silt ratios, the soil properties had a wide range of spatial dependence. as shown in Table 3, OM, N, Cu, Na, and K had strong spatial dependence, whereas Mn, Fe, Mg, Sand and Clay had moderate spatial dependence and OC, pH, P, Zn, Ca, Silt and CEC had weak spatial dependence, which could be due to the poor spatial distribution of these properties,

and thus additional research using a large scale sampling design to capture the spatial distribution of these variables is recommended. The maximum distance at which spatial dependence or autocorrelation exists was defined as the range value of a semi-variogram (Metwally *et al.*, 2019). From Table 3, soil properties ranged between 810 m for OC and OM and 3995 m for P and Ca. Soil properties with range values greater than the obtained range values have no spatial dependence.

Figures 2a and 2b show the model fit of soil Organic Carbon (SOC) and Soil Organic Matter (SOM), with the Stable and Gaussian models given as the best fits for the parameters. The SOC and SOM have nuggets of 0.00005 and 0.001 and sills of 0.05099 and 0.0501, respectively, with nugget to sill ratio of 0.001 and 0.02 (Table 3), given a strong spatial dependence that enhanced the prediction. The mean error (ME) for SOC and SOM is 0.026 and 0.024, the average standard error (ASE) is 0.18 and 0.18, and the root mean standard error (RMSE) is 0.17 and 18. For SOC and SOM, the mean standard error (MSE) is -0.110 and -0.091, and the root mean square standardized error (RMSSE) is 1.29 and 1,18, respectively. The cross-validation results show that the interpolation method was unbiased with an ME value of zero and the goodness of fit accuracy of the Kriging algorithm with ASE equals RMSE and RMSSE value of one, as shown in Table 3. Figure 4.4 shows the map of spatial distribution of carbon (ton/ha) in the biosphere, with the north-eastern part of the biosphere having 21.28 - 28.84 tons of carbon per hectare, while most of the north-west, central and South-western regions of the biosphere have 28.84-44.48 tons of carbon per hectare.

Table 3. Semi-variance Analysis of the Soil Properties

Variable	Model	Nugget	Partial Sill	Sill	Nugget/ Sill	SDC	Range (m)	ME	RMSE	MSE	RMSSE	ASE
OC (%)	Stable	0.01	0.05	0.05	0.01	S	810	-0.026	0.180	-0.11	1.29	0.17
OM (%)	Gaussian	0.01	0.049	0.05	0.020	S	810	-0.024	0.18	-0.09	1.18	0.18
pH	Exponential	0.116	0.000	0.12	1.000	W	3995	-0.003	0.36	-0.01	1.01	0.36
TN (%)	Stable	0.00	0.051	0.05	0.00	S	1520	-0.003	0.17	-0.01	1.1583	0.18
P (mg/kg)	Exponential	0.03	0.00	0.03	1.00	W	3995	-0.01	0.18	-0.03	1.015	0.17
Mn (mg/kg)	Gaussian	179.07	56.83	235.90	0.75	M	850	-0.79	14.46	-0.05	0.93	15.78
Fe (mg/kg)	Spherical	351.99	428.55	780.54	0.45	M	963	-0.57	28.053	-0.02	1.027	27.1
Cu (mg/kg)	Gaussian	0.29	2.69	2.99	0.10	S	850	-0.04	1.248	-0.01	1.073	1.39
Zn (mg/kg)	Gaussian	707.66	29.921	737.58	0.96	W	1339	-0.60	27.54	-0.02	0.98	28.20
Na (Cmol/kg)	Exponential	0.00	0.12	0.12	0.00	S	1150	-0.01	0.35	-0.03	1.107	0.31
K (Cmol/kg)	Exponential	0	0.18	0.18	0.00	S	2380	-0.03	0.46	-0.05	1.28	0.29
Mg (Cmol/kg)	Exponential	1.47	3.603	5.071	0.29	M	1739	-0.02	2.15	-0.01	1.08	2
Ca (Cmol/kg)	Exponential	16.27	0.00	16.27	1.00	W	3995	0.01	4.22	-0.01	1.01	4.19
Sand (%)	Exponential	22.57	13.23	35.80	0.63	M	1608	0.37	5.60	0.06	0.96	5.86
Clay (%)	Exponential	6.711	5.414	12.125	0.55	M	1765	-0.154	3.51	-0.039	1.054	3.32
Silt (%)	Exponential	13.91	3.097	17.00	0.82	W	1740	-0.16	4.05	-0.04	0.97	4.17
CEC (Cmol/kg)	Gaussian	21.31	3.69	25.00	0.85	W	1355	0.06	4.97	0.01	0.99	5.05

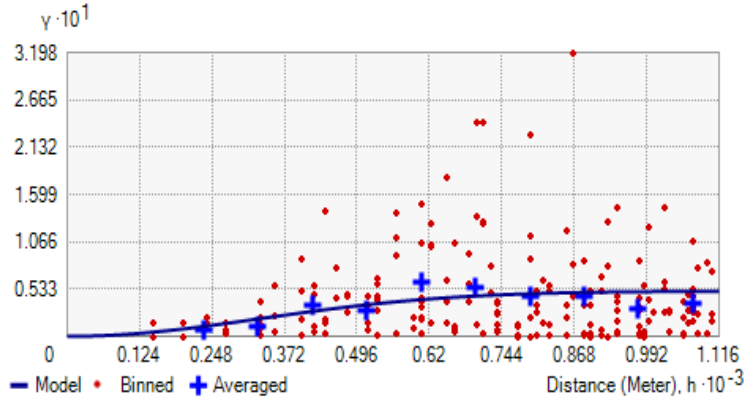

Figure 2a. Soil Organic Carbon (SOC)

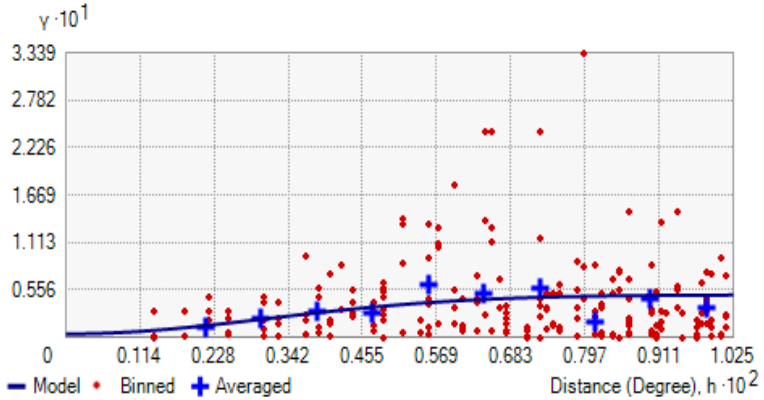

Figure 2b. Soil Organic Matter (SOM)

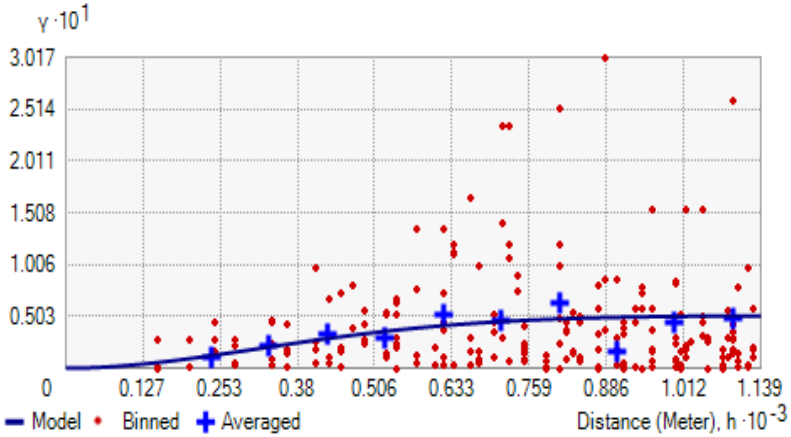

Figure 2c. Total Nitrogen (TN)

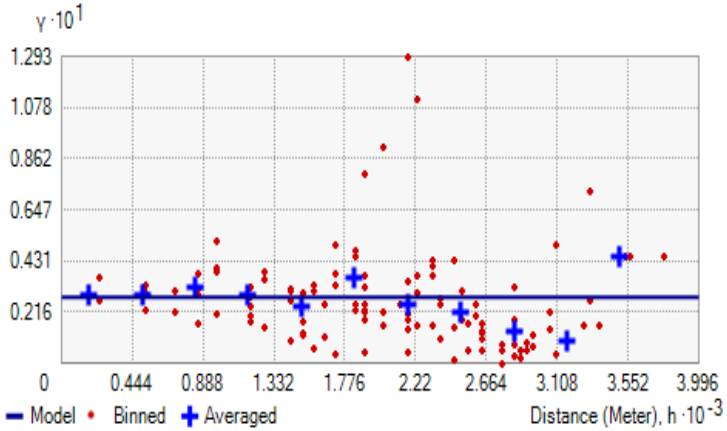

Figure 2d. Phosphorus (P)

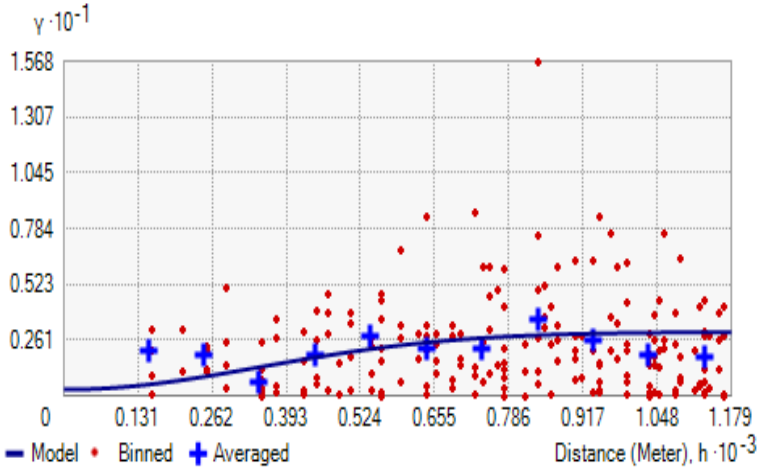

Figure 2e. Copper (Cu)

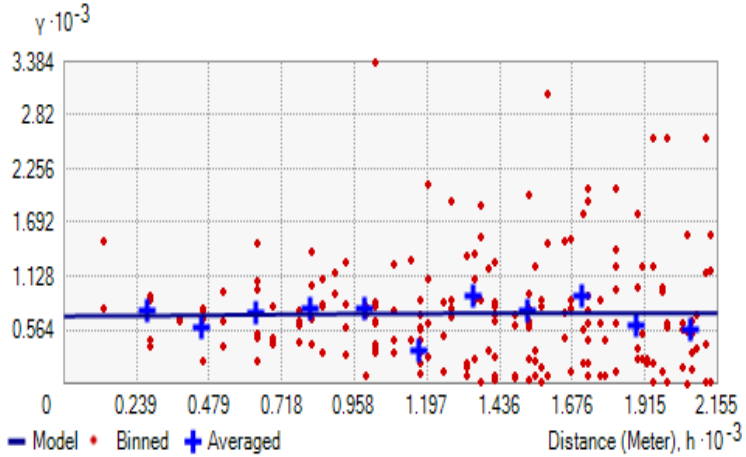

Figure 2f. Zinc (Zn)

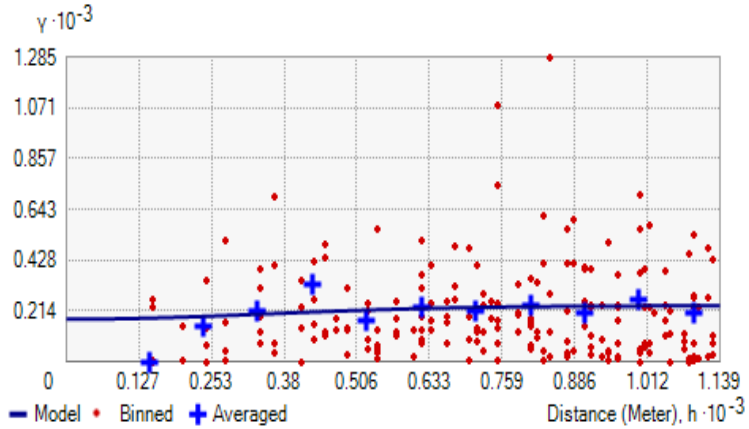

Figure 2g. Manganese (Mn)

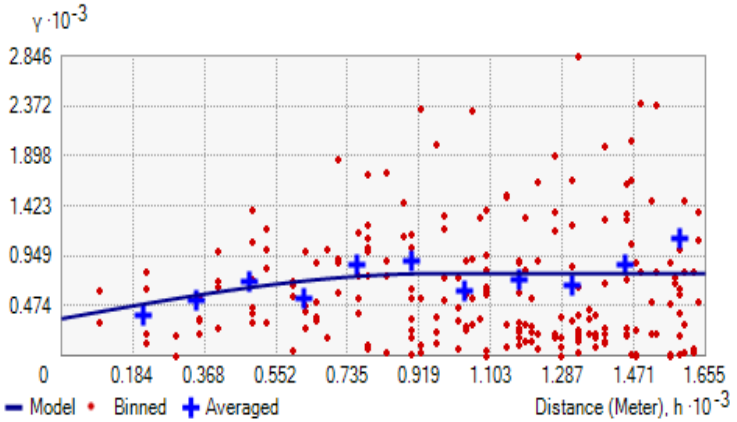

Figure 2h. Iron (Fe)

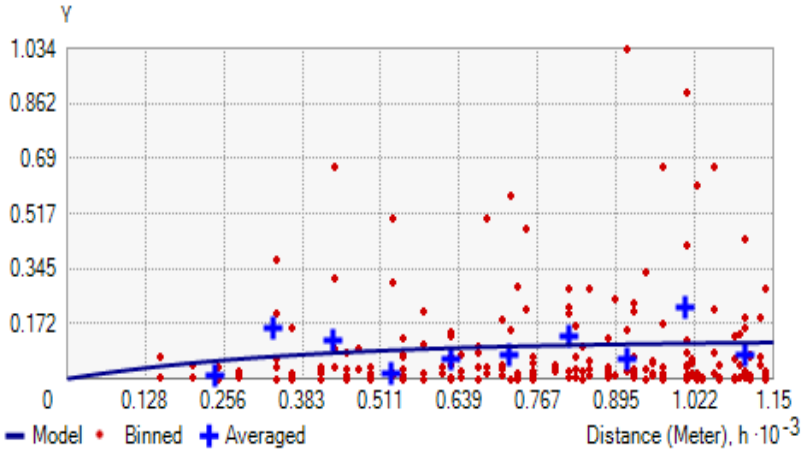

Figure 2i. Sodium (Na)

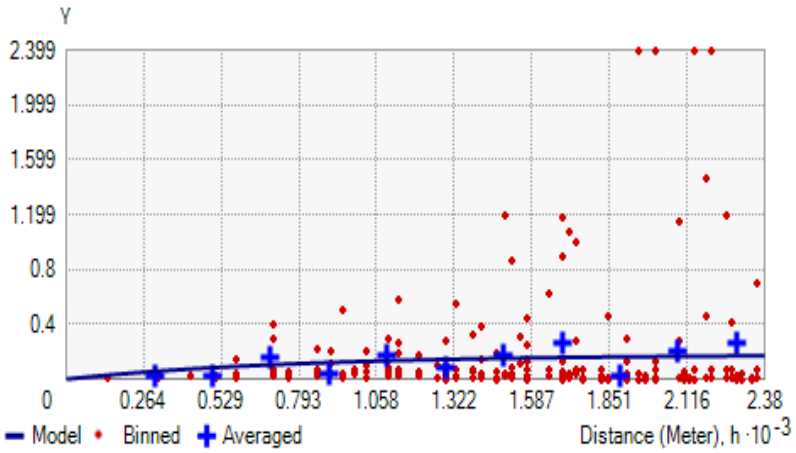

Figure 2j. Potassium (K)

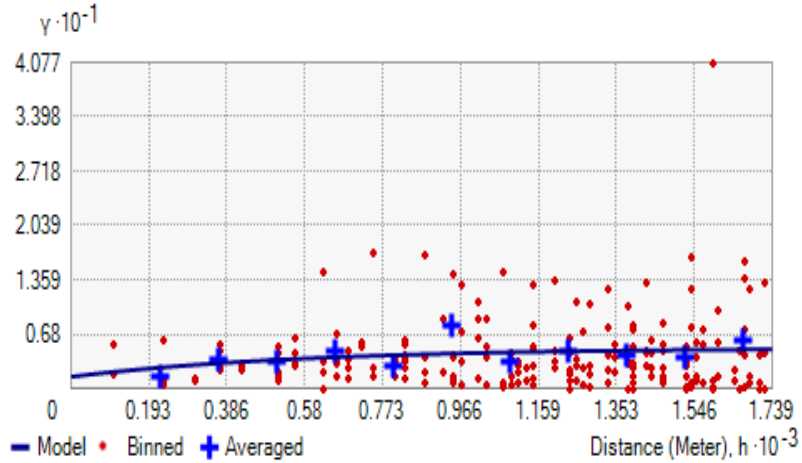

Figure 2k. Magnesium (Mg)

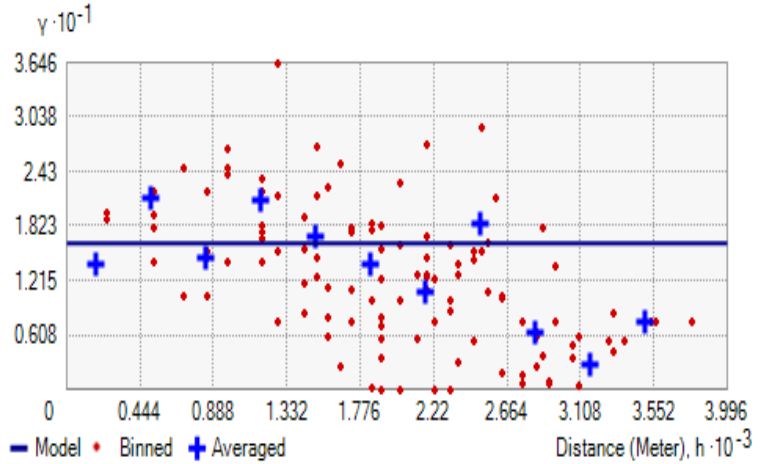

Figure 2l. Calcium (Ca)

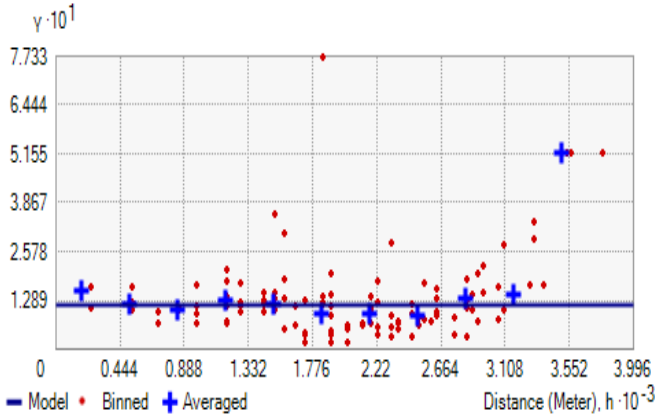

Figure 2m. Soil pH

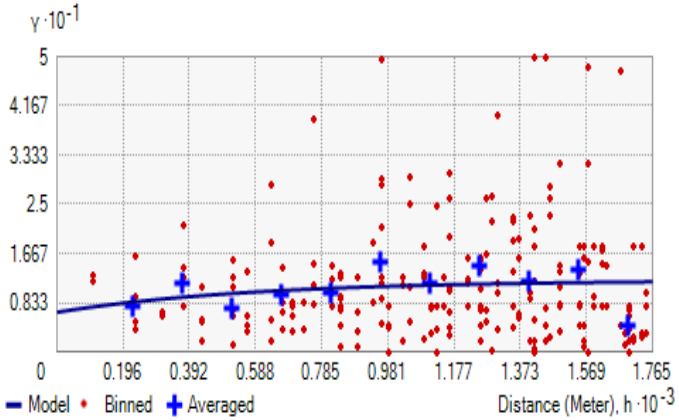

Figure 2n. Clay

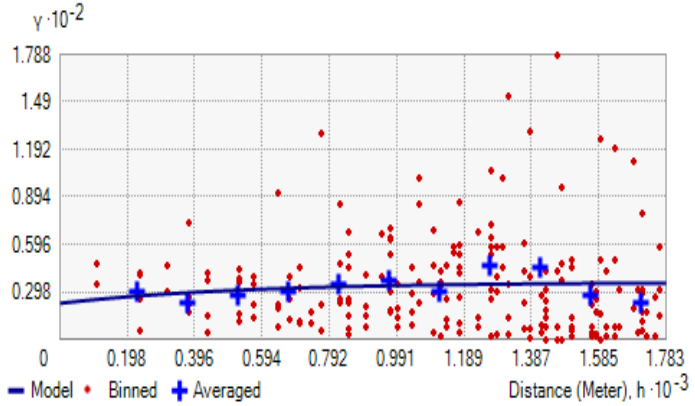

Figure 2o. Sand

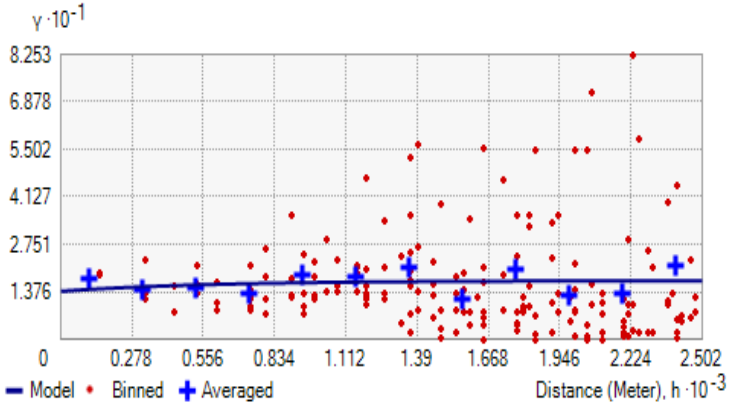

Figure 2p. Silt

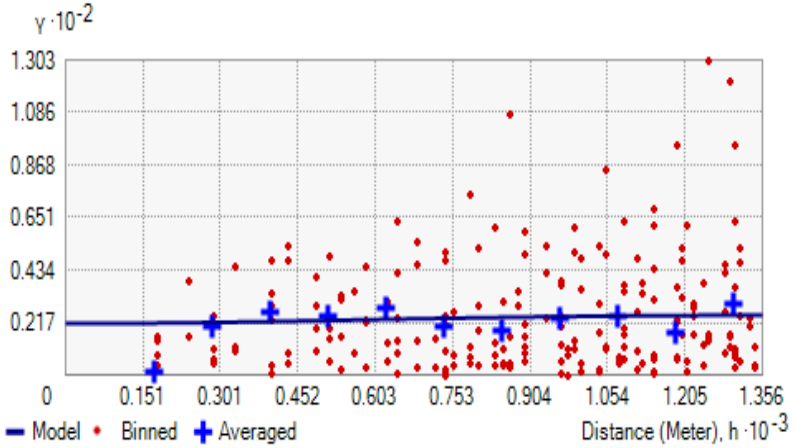

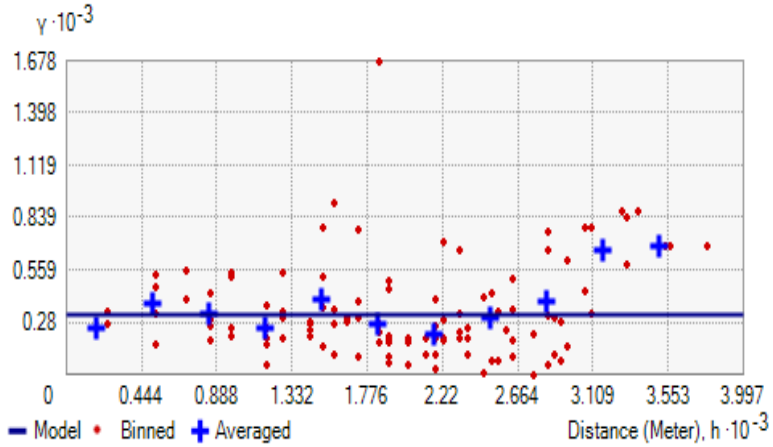

Figure 2q. Cation Exchange Capacity (CEC) Figure 2r. Soil Organic Carbon ton/ha

Figure 2. (a-r). Result of the Semi-variogram and fitted models for pH, SOC, SOM, N, P, Fe, Mn, Cu, Mg, Na, k, Zn, Sand, Silt, Clay and CEC

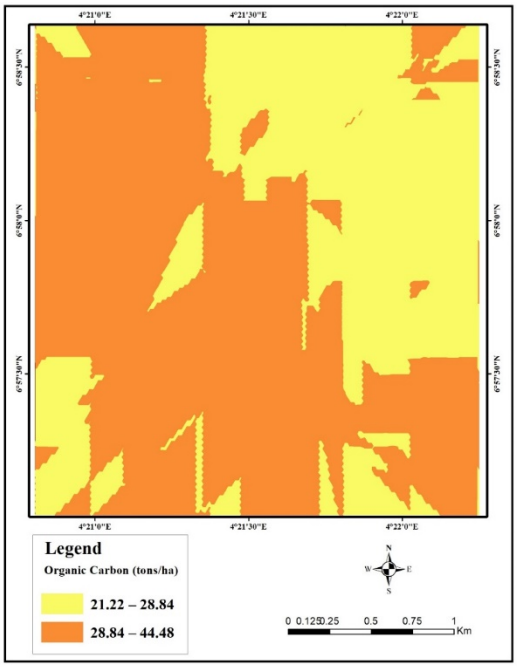

Figure 3. Spatial Distribution of Organic Carbon (ton/ha)

Figure 4 shows the spatial distribution maps of SOC and SOM. In the north-east and central parts of the Omo biosphere, the percentage of soil organic carbon was 0.6-1.05 % and organic matter had the lowest value (1.03-1.87) in the area. It shows the positive correction between organic carbon and organic matter, with the two maps looking almost the same due to the spatial distribution of soil properties. Stable and exponential models gave the best fit for Total Nitrogen (NT) and Available Phosphorus (AP) (Table 3). Figures 2c and 2d depict the model fit for nuggets of 0 and sills of 0.051 and 0.027 with nugget to sill ratio of 0 and 1 (Table 3), respectively, given a strong and weak spatial dependence for the two soil properties. The cross-validation technique performed for SOC and SOM has a mean error (ME) of 0.002, 0.004, average standard error (ASE) of 0.18, 0.17, Root Mean Standard Error (RMSE) 0.17, 18, Mean Standard Error (MSE) -0.008, -0.027 and Root Mean Square Standardized Error (RMSSE) of 1.15, 1,01 for TN and AP, respectively. The cross-validation results show that the interpolation method was unbiased with an ME value of zero and the goodness of fit accuracy of the Kriging algorithm with an ASE equals RMSE and RMSSE value of one, as shown in Table 3.

The analysis gave an output of the spatial distribution maps of TN and AV in Figure 5. The spatial distribution map of total nitrogen shows the same trend as SOC and SOM, while the entire biosphere has an AP of 4.11-5.22 mg/kg with an insignificant area in the South-west of the map having 3.51-4.11 mg/kg of AP.

Figures 2e and 2f show the model fit of Copper (Cu) and Zinc (Zn) with the Gaussian models given the best fit the parameters. Cu and Zn have nuggets of 0.294, 707.6 and sills of 2.990, 737.9 with nugget to sill ratio of 0.10 and 0.96 (Table 3) respectively. Cu has a strong spatial dependence, as seen in the graph, rising from its nugget of 0.294 to its sill of 2.99, while Zn has a weak spatial dependence. The cross-validation technique performed for Cu and Zn showed that the interpolation method was unbiased based on ME, ASE, RMSE and RMSSE values (Table 3). Figure 6 shows the map of the spatial distribution of Cu (mg/kg) and Zn (mg/kg) in the biosphere, with the northern and central part of the Omo biosphere having the highest concentration of Cu (4.7-6.7 mg/kg) and the South-western and eastern parts having the lowest concentration of Cu (0.8-2.8 mg/kg). 72.62-

91.63 mg/kg of Zn was concentrated in the Omo biosphere.

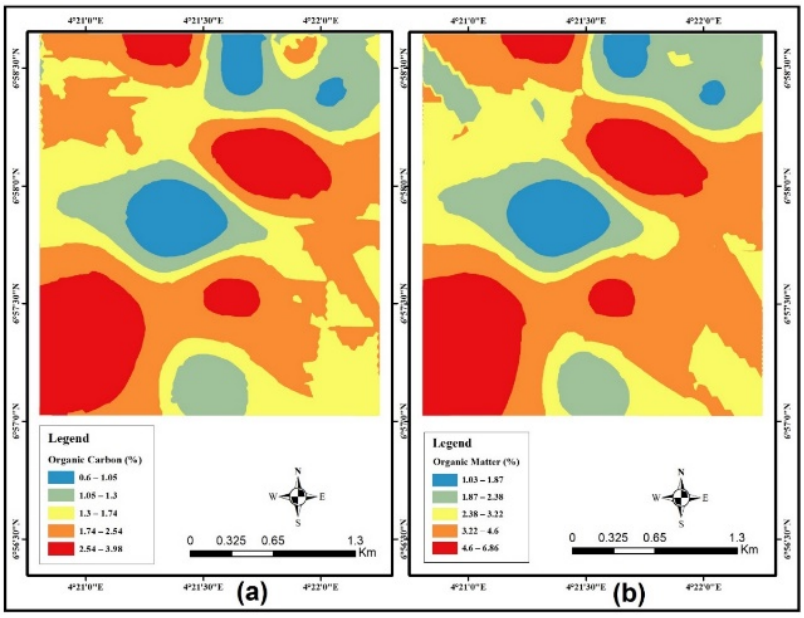

Fig. 4. Spatial Distribution of Organic Carbon (a) and Organic Matter (b).

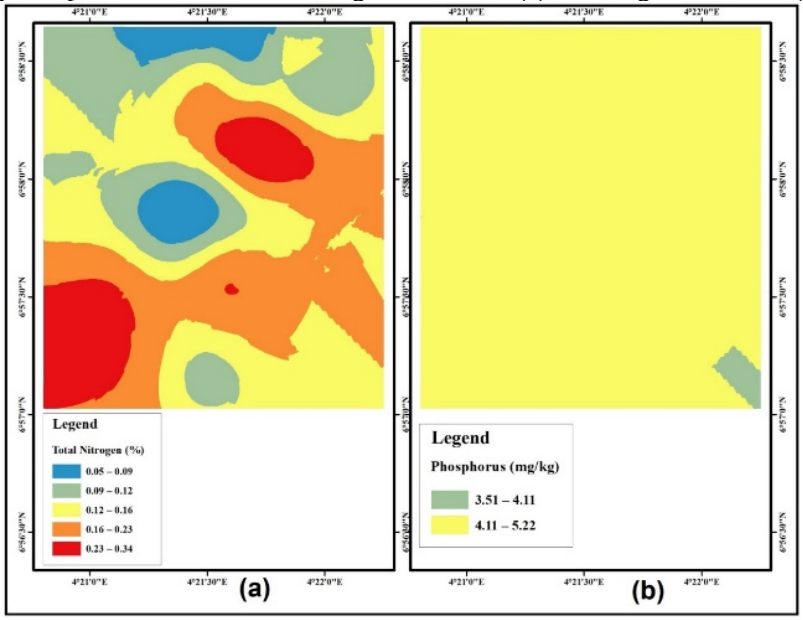

Fig. 5. Spatial Distribution of Nitrogen (a) and Phosphorus (b)

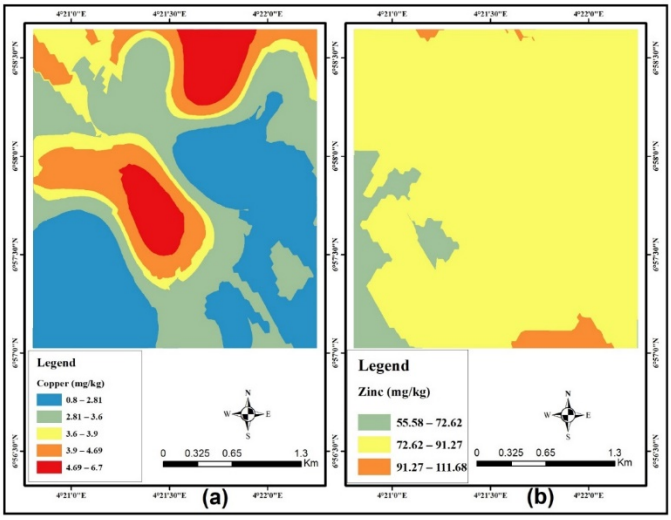

Figure 6. Spatial Distribution of Copper (a) and Zinc (b)

The Gaussian and Spherical models were the best fit for Manganese (Mn) and Iron (Fe), as shown in Figures 4.3g and 4.3h. The nuggets-to-sills ratio of 0.75 and 0.45 (Table 4.12) showed a moderate spatial dependence, with the spatial distribution map of showing concentrations of Mn of 29.65 - 40.66 mg/kg in the north and south of the Omo biosphere while the central portion has Mn between 19.6 - 29.65 mg/kg. The north-east and South-western part of the Omo biosphere has Fe concentration of 58.8-81.98 mg/kg, 25.51 - 40.29 mg/kg while the remaining part of the biosphere has Fe concentration of 40.29 - 81.98 mg/kg (Figure 7). Both Sodium (Na) and Potassium (K) have a strong dependence, with the exponential being the best fit for both. They have a nuggets-to-sills ratio of 0, 0 and 0.119, 0.179 respectively, and the cross-validation technique used for Na and K revealed that the interpolation method was unbiased based on ME, ASE, RMSE and RMSSE values (Table 3). The spatial distribution maps (Figure 8) improve the prediction by showing the concentration of Na across the Omo biosphere ranging from 0.31-0.8 to 3.3-8.6 Cmol/kg, with 0.94-1.4 covering the largest area. K concentration ranges from 0.0002-0.0003 to 0.0021-0.031 Cmol/kg. The lowest concentration was in the north and south east while highest was at the South Western part of the biosphere. The exponential model was the best for Magnesium (Mg) and Calcium (Ca). The Mg has a moderate spatial dependence with nugget to sill ratio of 0.29 while Ca has a weak spatial dependence with nugget to sill ratio of 1. The cross-validation technique performed for Cu and Zn showed that the interpolation method was unbiased based on ME, ASE, RMSE and RMSSE values (Table 3). Figure 9 showed the spatial distribution maps Mg and Ca. From north west to south east of the biosphere Mg concentration was 2.88-4.58 Cmol/kg with the highest of 7.65 - 9.79 Cmol/kg at the South Western part of the biosphere. The biosphere has Ca concentration of 8.39-11.29 Cmol/kg. Sand, Clay and Silt have moderate, moderate and weak spatial dependence with the exponential model as best fit for the parameters.

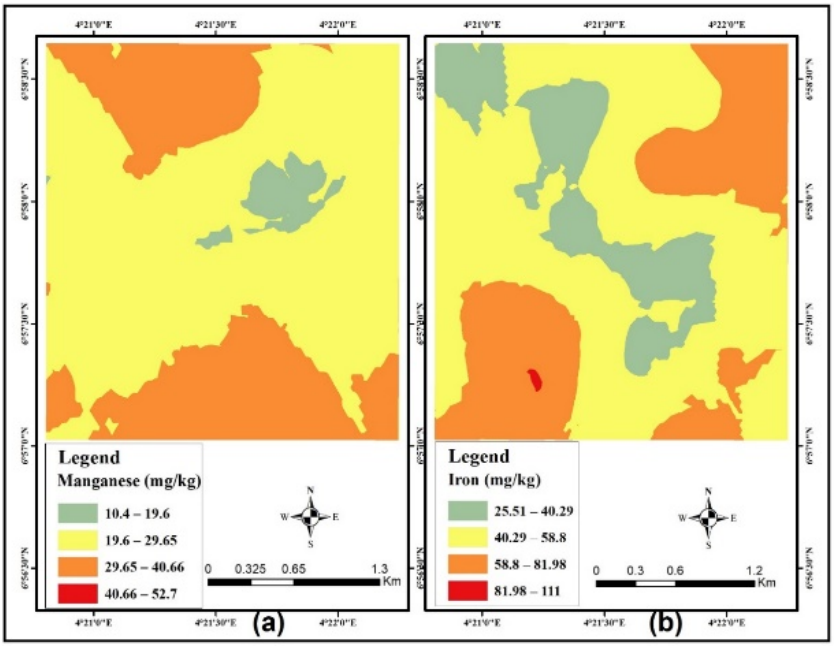

Figure 7. Spatial Distribution of Mn (a) and Iron (b).

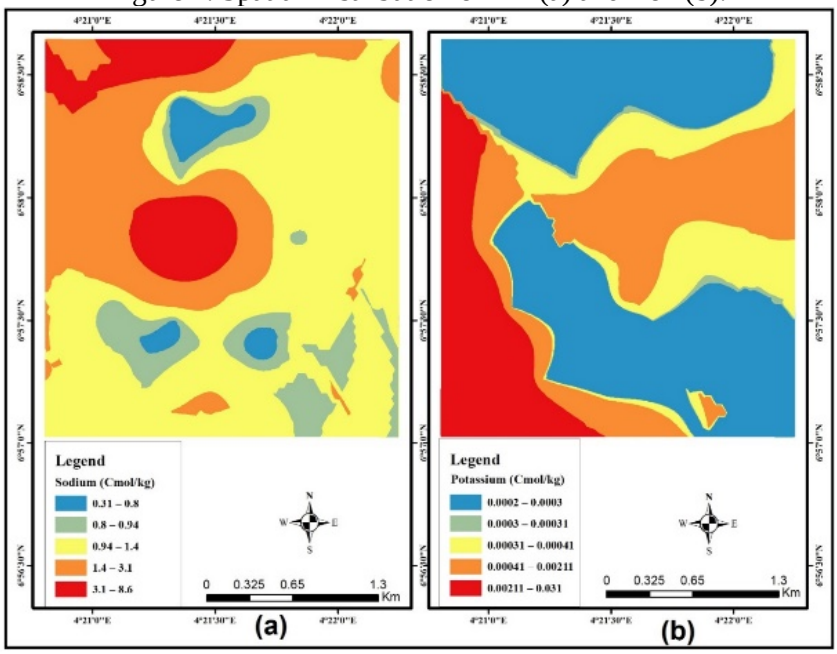

Figure 8. Spatial Distribution of Sodium (a) and Potassium (b)

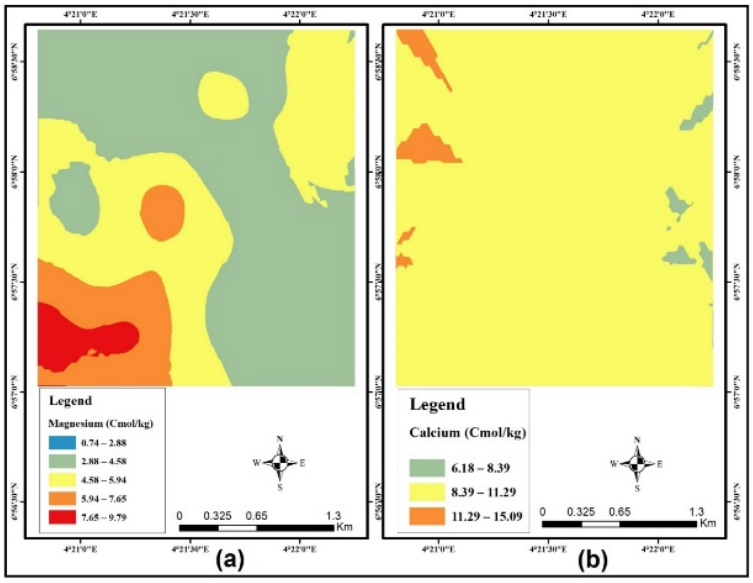

Fig. 9. Spatial Distribution of Mg (a) and Calcium (b)

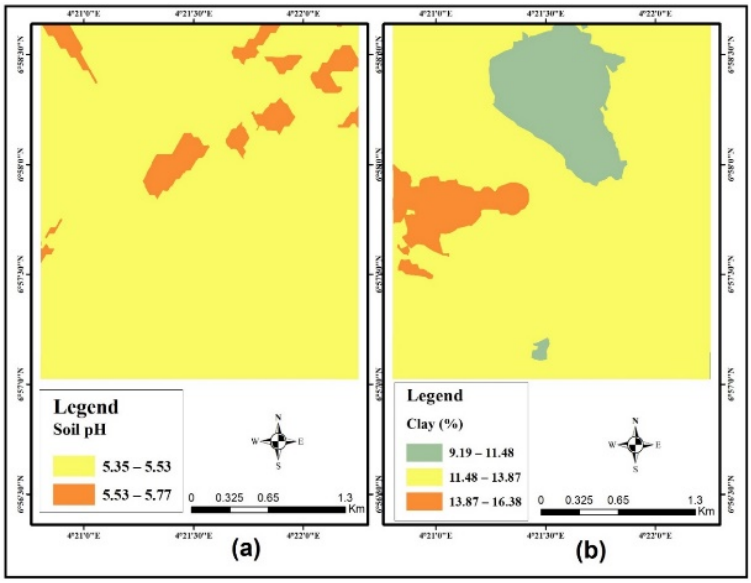

Fig. 10. Spatial Distribution of Soil pH (a) and Clay (b)

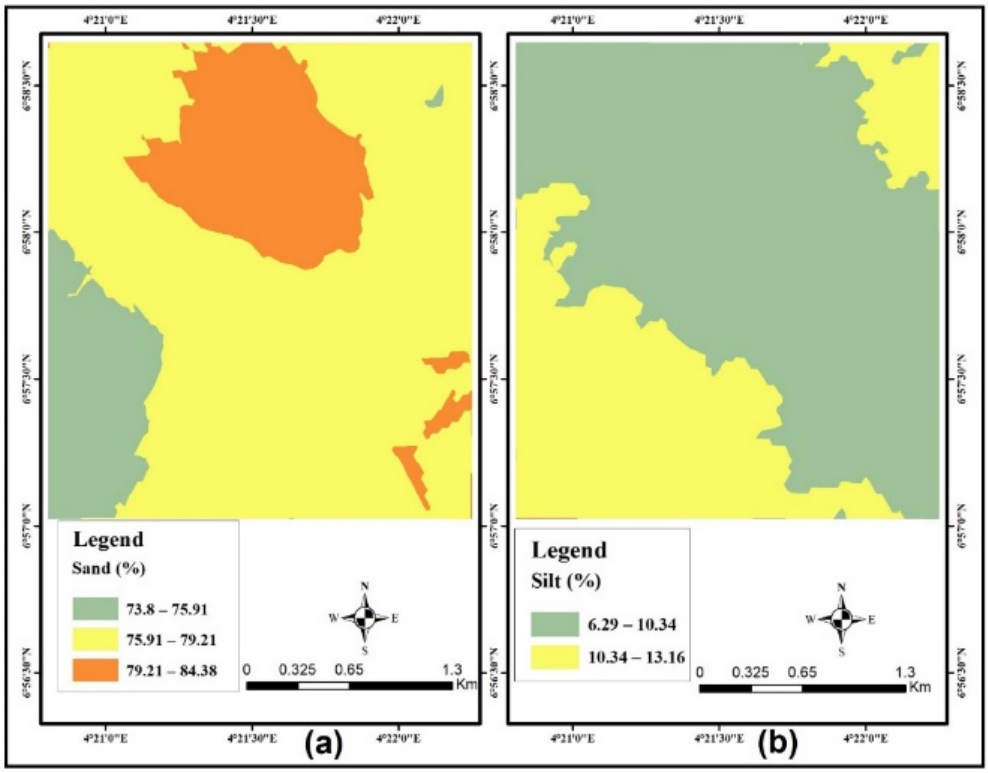

Fig. 12. Spatial Distribution of Sand (a) and Silt (b)

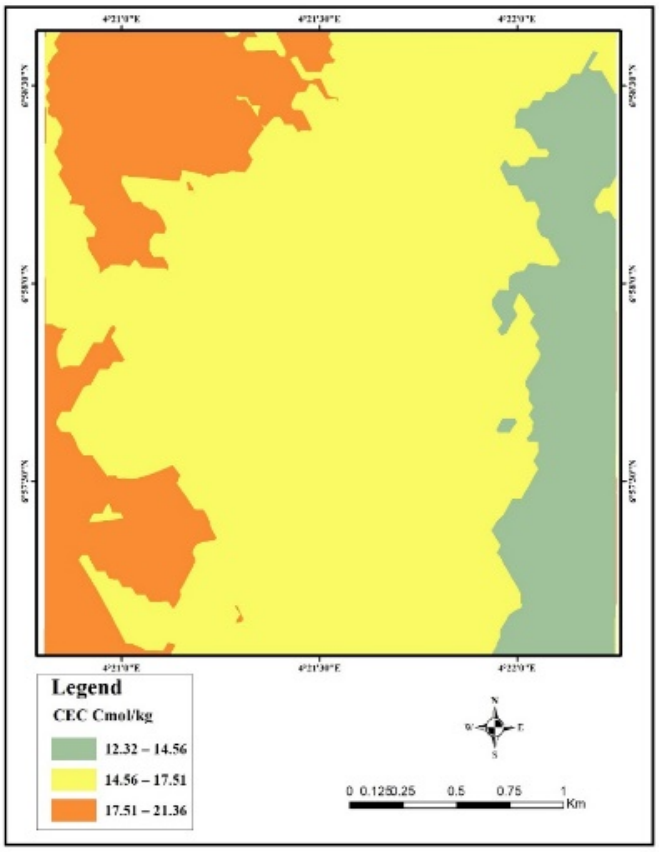

Fig. 13. Spatial Distribution of CEC

Conclusion

The results reported in this study revealed the high potential of that soil organic carbon has in mitigating the impacts of climate change. The soil variability shows the high uptake of micronutrient due the acidity of the soil as revealed from the result. There is wide range of spatial dependency in the soil property as some are strongly, moderately and weakly dependent. Under half of the semi-variogram range value, soil samples should be separated. By obtaining samples at intervals less than half of the acquired range values of the researched soil properties, one may utilise the range values for soil properties to schedule future soil sampling for geostatistical research. Thus, additional research using a large-scale sampling design to capture the spatial distribution of these variables is recommended. Both directly and indirectly, climate change can impact soil properties. The immediate consequences include changing soil moisture and temperature regimes, altered organic carbon transformations, and altered nutrient cycling, as well as higher soil erosion rates brought on by the frequency of heavy rainfall events. A crucial step in the lowering emissions and increasing aboveground biomass is by monitoring soil degradation through thorough soil mapping. The consequence of improper land use on the soil management and regeneration of plants may be found through soil mapping.

Acknowledgement

This work is supported financially by the African Union under the Pan African University scholarship. Forestry Research Institute of Nigeria is also acknowledged for granting permission to use Omo Strict Nature Reserve (Omo Biosphere Reserve) for this study

References

Adedeji, O.H., Tope-Ajayi, O.O., & Abegunde, O.L. (2015). 'Assessing and Predicting Changes in the Status of Gambari Forest Reserve, Nigeria Using Remote Sensing and GIS Techniques'. *Journal of Geographic Information System*, 7, 301-318.

Ahmed, I.U. (2018) Forest Soil C: Stock and Stability under Global Change. New Perspectives in Forest Science. http://dx.doi.org/10.5772/intechopen.74690

Bhunia GS, Shit PK, Maiti R. (2016) Comparison of GIS-based interpolation methods for spatial distribution of soil organic carbon. Journal of the Saudi Society of Agricultural Sciences.

Bivand, R.S.; Pebesma, E.J.; Gomez-Rubio, V. Applied Spatial Data Analysis with R; Springer: New York, NY, USA, 2008.

Buol, S.W., R.J. Southard, R.C. Graham, and P.A. McDaniel. *Soil Genesis and Classification*. 5th edition. Iowa State Press. A Blackwell Publishing Company, 2003, pp. 3-34.

Cambardella, C.A.; Moorman, T.B.; Parkin, T.; Karlen, D.; Novak, J.; Turco, R.; Konopka, A. (1994) Field-scale variability of soil properties in central Iowa soils. Soil Sci. Soc. Am. J.58, 1501–1511.

Chen, S., Wang, W., Xu, W., Wang, Y. et al., (2018) Plant diversity enhances productivity and soil carbon storage. PNAS vol. 115 no. 16 4027–4032.

Cheng L, Leavitt SW, Kimball BA, Pinter Jr PJ, Ottman MJ, Matthias A, Wall GW, Brooks T, Williams DG, Thompson TL. Dynamics of labile and recalcitrant soil carbon pools in a sorghum free-air CO2 enrichment (FACE) agro-ecosystem. Soil Biology & Biochemistry. 2007;39:2250-2263

Cressie, N. Statistics for Spatial Data, revised ed.; John Wiley & Sons: New York, NY, USA, 1993.

Esu, I.E. (1991). Detailed Soil Survey of NIHORT Farm at Bunkure, Kano State, Nigeria. Institute for Agricultural Research, Ahmadu Bello University, Zaria

FAO (2015). Soils are the foundation for vegetation. International Year of Soils. *fao.org/soils-2015*

Goovaerts, P. Geostatistics for Natural Resources Evaluation; Oxford University Press: New York, NY, USA, 1997.

Goovaerts, P. Geostatistics in soil science: State-of-the-art and perspectives. Geoderma 1999, 89, 1–45.

Hengl, T. A Practical Guide to Geostatistical Mapping; Tomislav Hengl: Amsterdam, The Netherlands, 2009.

Intergovernmental Panel on Climate Change (IPCC). Climate Change 2007: Working Group I, Fourth Assessment Report. Technical Summary. Geneva, Switzerland. 2007

Kiehl JT, Trenberth KE. Earth's annual global mean energy budget. Bulletin of the American Meteorological Society. 1997;78(2):197-208

Kirschbaum, M. U. F. (2000). Will Changes in Soil Organic Carbon Act as a Positive or Negative Feedback on Global Warming? Biogeochemistry 48 (1), 21–51. doi:10.1023/a:1006238902976

Krasilnikov, P.; Carré, F.; Montanarella, L. (2008). Soil Geography and Geostatistics; Office for Official Publications of the European Communities: Luxembourg.

Lal, R. (2004). Soil Carbon Sequestration Impacts on Global Climate Change and Food Security. Science 304 (5677), 1623–1627. doi:10.1126/ science.1097396

Larinde, S.L., & Olasupo, O.O. (2011). 'Socio-Economic Importance of Fuelwood Production in Gambari Forest Reserve Area, Oyo State, Nigeria'. *Journal of Agriculture and Social Research (JASR)*, 11.

Lark RM. (2000) Estimating variograms of soil properties by the method-of-moments and maximum likelihood. European Journal of Soil Science. 51:717–728.

Li, J.; Heap, A.D. A Review of Spatial Interpolation Methods for Environmental Scientists; Geoscience Australia: Canberra, Australia, 2008.

Li, J.; Heap, A.D. Spatial interpolation methods applied in the environmental sciences: A review. Environ. Model. Softw. 2014, 53, 173–189.

Luo Y, Zhou X. Soil Respiration and the Environment. Elsevier; 2006. pp. 25-26

Makinde, E. O., Womiliju, A. A. & Ogundeko, M. O (2017) The geospatial modelling of carbon sequestration in Oluwa Forest, Ondo State, Nigeria, European Journal of Remote Sensing, 50:1, 397-413, DOI: 10.1080/22797254.2017.1341819

Metwally, M.S., Shaddad, S.M., Liu, M., et al (2019) Soil Properties Spatial Variability and Delineation of Site-Specific Management Zones Based on Soil Fertility Using Fuzzy Clustering in a Hilly Field in Jianyang, Sichuan, China. Sustainability 11, 7084; doi:10.3390/su11247084 www.mdpi.com/journal/sustainability

National Oceanic and Atmospheric Administration (NOAA). Earth System Research Laboratory, GMD, The Global Greenhouse Gas Reference. Hawaii, United States: NOAA-Mauna Loa Observatory. 2017. Available from: https://www.esrl.noaa.gov/gmd/ccgg/trends

Okali, D.U.U. and Ola-Adams, B.A. 1987. Tree population changes in treated rain forest at Omo Forest Reserve, Nigeria. *Journal of Tropical Ecology* 3,291-313.

P.I. Ezeaku. *Methodologies for Agricultural land-use planning. Sustainable soil management and productivity*. Great AP Express Publishers Ltd, Nsukka, 2011, pp. 1–4.

Pebesma, E.J. The role of external variables and GIS databases in geostatistical analysis. Trans. GIS 2006, 10, 615–632.

Reza SK, Sarkar D, Baruah U, Das TH (2010). Evaluation and comparison of ordinary kriging and inverse distance weighting methods for prediction of spatial variability of some chemical parameters of Dhalai district, Tripura. Agropedology. 20(1):38–48.

Tripathi R, Nayak AK, Shahid M, Raja R, Panda BB, Mohanty S, *et al*. (2015) Characterizing spatial variability of soil properties in salt affected coastal India using geostatistics and kriging. Arabian Journal of Geosciences. 8(12):10693–10703.

Venteris ER, Basta NT, Bigham JM, Rea R. (2013) Modeling spatial patterns in soil arsenic to estimate natural baseline concentrations. Journal of Environmental Quality. 43(3):936–946.

Wang X, Li Y, Duan Y, Wang L, Niu Y, Li X and Yan M (2021) Spatial Variability of Soil Organic Carbon and Total Nitrogen in Desert Steppes of China's Hexi Corridor. Front. Environ. Sci. 9:761313. doi: 10.3389/fenvs.2021.761313

Yang, Y., Zhu, J., Zhao, C., Liu, S., Tong, X., (2011). The spatial continuity study of NDVI based on Kriging and BPNN algorithm. Math. Comput. Model. 54, 1138–1144. Dc